Supporting Information

Mechanical Properties of Metal Oxide Aerogels

*Albrecht Benad, Florian Jürries†, Birgit Vetter†, Benjamin Klemmed, René Hübner††, Christoph Leyens†, Alexander Eychmüller**

Physical Chemistry, Technische Universität Dresden, Bergstraße 66b, 01062 Dresden, Germany
† Materials Technology, Technische Universität Dresden, Helmholtzstraße 7, 01062 Dresden, Germany
†† Institute of Ion Beam Physics and Materials Research, Helmholtz-Zentrum Dresden-Rossendorf, Bautzner Landstraße 400, 01328 Dresden

Corresponding author: *E-Mail: alexander.eychmueller@chemie.tu-dresden.de

Annealed alumina aerogels

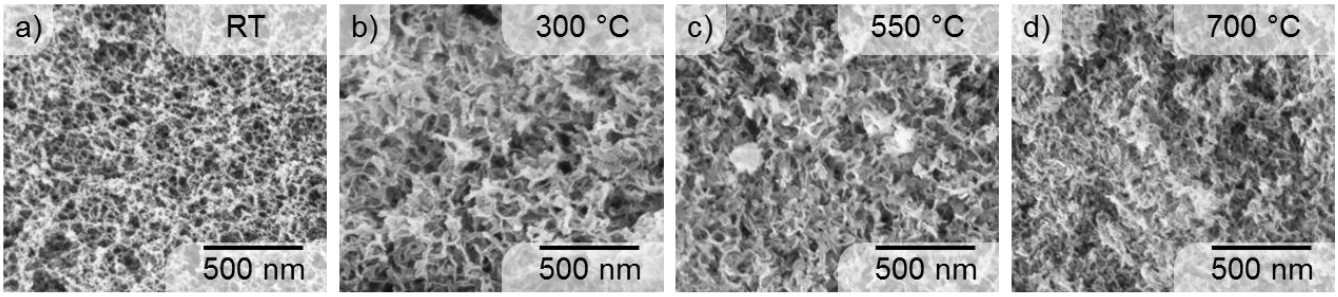

Figure S1: SEM images of sheet-like morphology of alumina aerogels which retained after each heat treatment. a) room temperature (RT), b) 300 °C, c) 550 °C, d) 700 °C

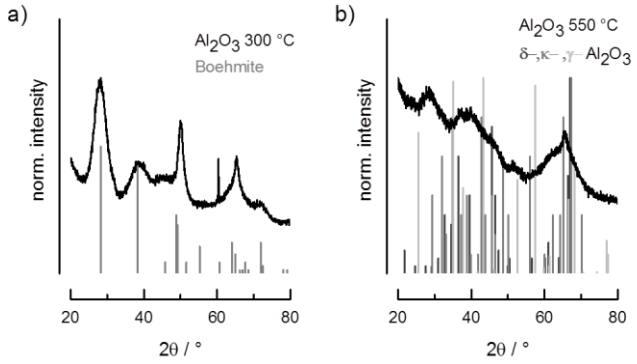

Figure S2: XRD of alumina aerogels annealed a) at 300 °C with (pseudo-)boehmite structure and b) at 700 °C with mixed aluminum oxide structure.

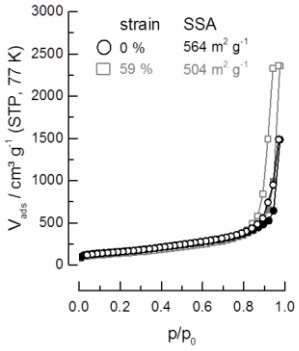

FigureS3: 81 points isotherms of alumina aerogels annealed at 300 °C before and after pressure test (strain 59 %). The porous networks represent a mixture of typ II and IV isotherm. Both isotherms show a similar curve shape, but adsorbed volume after densification is increased due to the compression of former large macropores and since that are accessible for the nitrogen physisorption. Hence, network structure retained intact after compression.

Table S1. Annealed alumina aerogels and characterization; Young's modulus E, density ρ, specific Young's modulus E/ρ, specific surface area SSA, total pore volume TPV (at $p/p_0 = 0.95$), shrinkage and compressive strength at 50% strain CS50.

annealing T / °C	E / MPa	ρ / mg mL^{-1}	E/ρ / MPa mL g^{-1}	SSA / m^2 g^{-1}	TPV / cm^3 g^{-1}	shrinkage / %	CS50 / MPa
RT	4.6 ± 0.6	61 ± 4	72 ± 6	751	1.21	40.8 ± 1.0	1.0
300	6.1 ± 0.6	60 ± 6	103 ±1 6	564	0.6	44.8 ± 1.2	1.4
550	7.4 ± 0.1	79 ± 4	95 ± 5	503	0.7	50.5 ± 0.5	2.1
700	12.2 ± 1.2	86 ± 2	142 ± 13	477	0.8	53.9 ± 0.2	-

Table S2. Chosen references listed with mechanical properties and densities of published inorganic aerogels.

reference	material	E / MPa	ρ / mg mL^{-1}	E/ρ / MPa mL g^{-1}
Fricke[15]	SiO_2	3,25	158	21
Alaoui[S1]	SiO_2	6,5	220	30
Poco[29]	Al_2O_3	0,55	37	15
Zu[30]	Al_2O_3	11,4	181	63
Zu[12]	Al_2O_3	1,7	93	18
	Al_2O_3-Al_2O_3	6,7	143	47
	ZrO_2-ZrO_2	10,7	245	44

Single compound aerogels

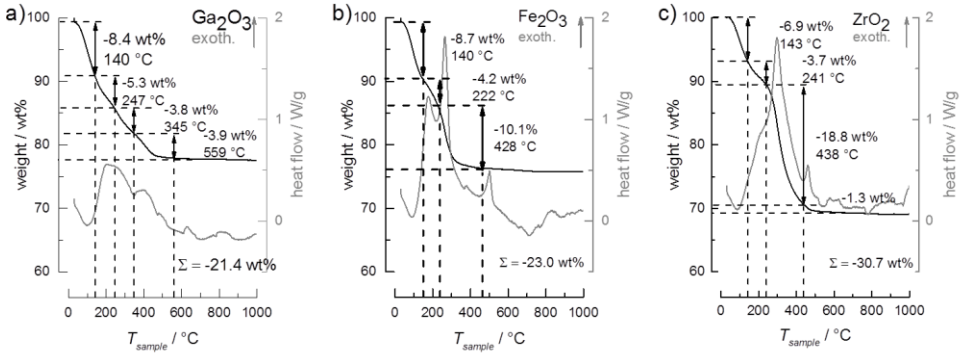

Figure S4: DTA-TG measurements of a) gallia, b) iron oxide and c) zirconia aerogels

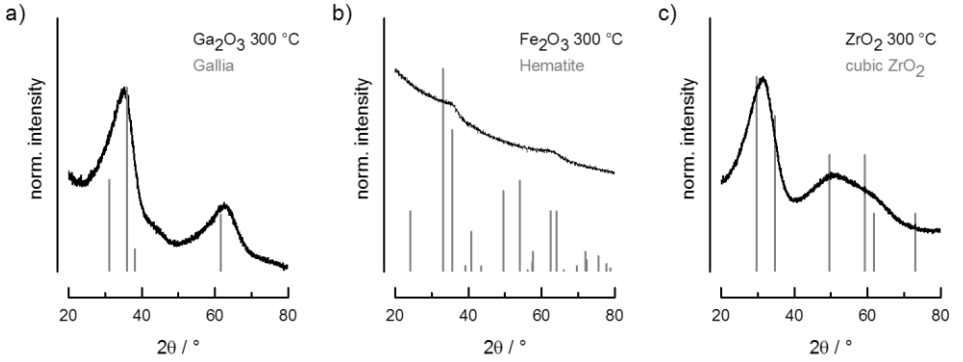

Figure S5: XRD patterns of mainly amorphous of a) gallia, b) iron oxide and c) zirconia aerogels.

Table S3. Single compound aerogels and characterization; Young's modulus E, density ρ, specific Young's modulus E/ρ, specific surface area SSA, total pore volume TPV (at $p/p_o = 0.95$), shrinkage.

material	E / MPa	ρ / mg mL^{-1}	E/ρ / MPa mL g^{-1}	SSA / m^2 g^{-1}	TPV / cm^3 g^{-1}	shrinkage / %	strain / %
Al2O3	2.9 ± 0.2	49.8 ± 0.5	58 ± 3	709	1.25	29.2 ± 0.2	>50
Ga2O3	0.36 ± 0.02	65.1 ± 1.5	5.5 ± 1.8	327	0.54	23.1 ± 0.5	15.3 ± 1.2
Fe2O3	8.1 ± 0.5	140.7 ± 14.7	58 ± 3	357	0.69	45.3 ± 0.5	6.1 ± 1.1
ZrO2	10.7 ± 0.8	202.2 ± 17.5	53 ± 4	351	0.89	42.3 ± 2.1	4.3 ± 1.0

Mixed aerogels

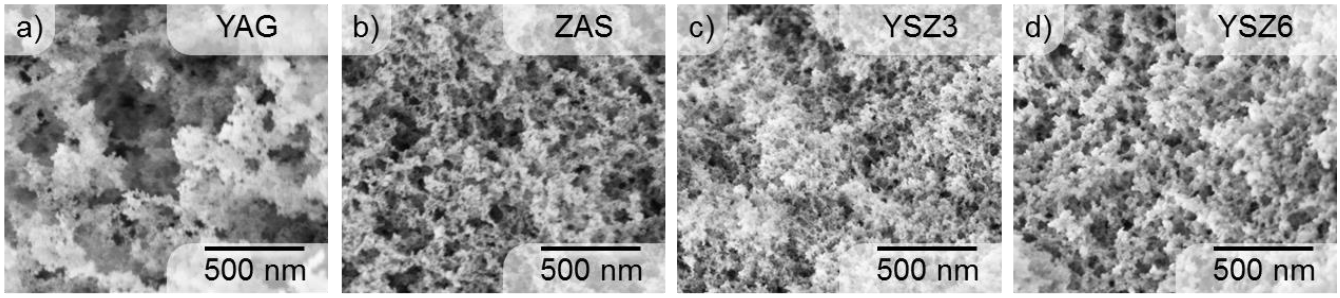

Figure S6: SEM images of mixed aerogels after annealing at 300 °C; a) yttrium aluminum garnet (YAG), b) zinc aluminum spinel, c) yttrium stabilized zirconium oxide 3 at% Y (YSZ3), d) yttrium stabilized zirconium oxide 6 at% Y (YSZ6)

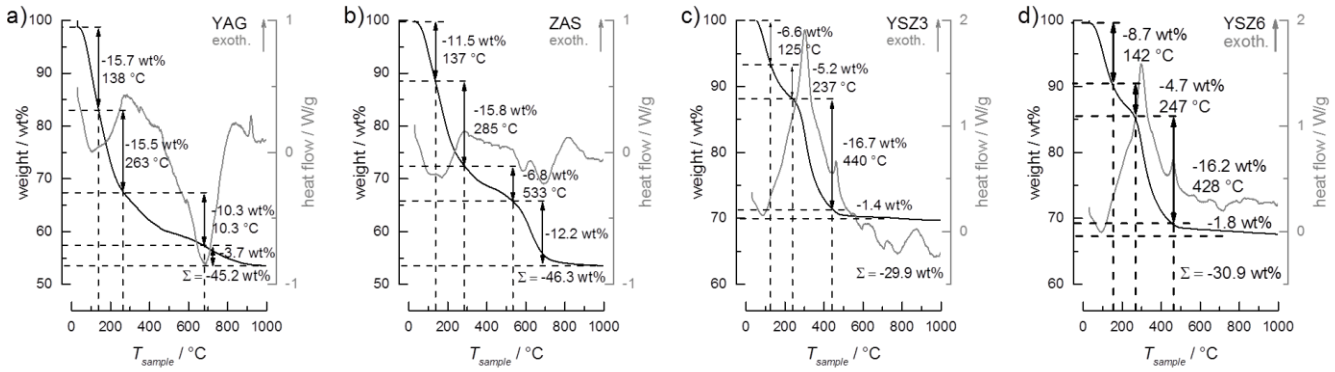

Figure S7: DTA-TG measurements of mixed aerogels; a) yttrium aluminum garnet (YAG), b) zinc aluminum spinel, c) yttrium stabilized zirconium oxide 3 at% Y (YSZ3), d) yttrium stabilized zirconium oxide 6 at% Y (YSZ6)

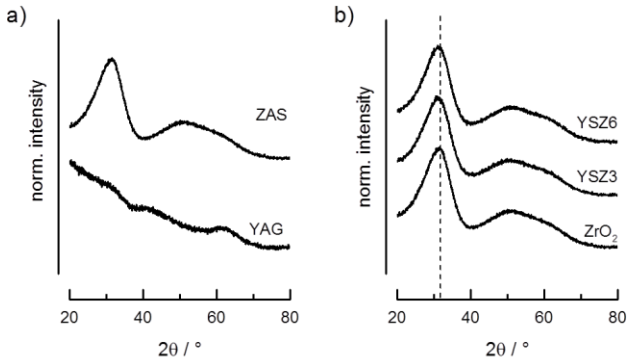

Figure S8: XRD patterns of amorphous mixed aerogels; a) yttrium aluminum garnet (YAG) and zinc aluminum spinel, as well as b) zirconia yttrium stabilized zirconium oxide 3 at% Y (YSZ3), yttrium stabilized zirconium oxide 6 at% Y (YSZ6) which show a slightly shift of reflections to lower angles due to a lattice contraction.

Table S4. Mixed aerogels and characterization, Young's modulus E, density ρ, specific Young's modulus E/ρ, specific surface area SSA, total pore volume TPV (at $p/p_o = 0.95$), shrinkage.

material	E / MPa	ρ / mg mL^{-1}	E/ρ / MPa mL g^{-1}	SSA / m^2 g^{-1}	TPV / cm^3 g^{-1}	shrinkage / %	strain / %
YAG	0.07	31.3	2.1	366	0.99	11.9	>50
ZAS	1.2 ± 0.2	71.2 ± 3.3	17 ± 2	372	0.92	33.0 ± 0.8	5.8 ± 0.4
YSZ3	5.6 ± 1.6	169.4 ± 16.7	33 ± 6	359	0.72	39.7 ± 1.1	4.7 ± 0.2
YSZ6	4.7 ± 0.2	158.4 ± 2.8	30 ± 1.0	356	0.67	38.6 ± 0.4	3.5 ± 0.7

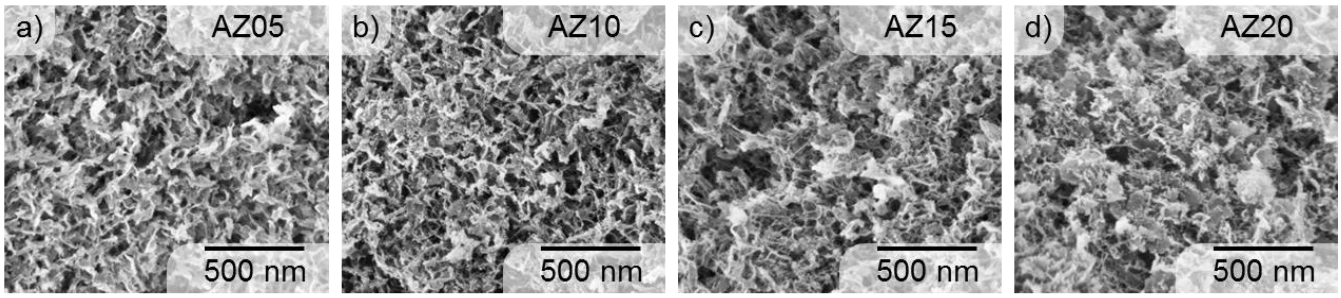

Figure S9: SEM images after annealing at 300 °C. Sponge-like morphology occurs increasingly due to Zr content from 0 to 20 at% Zr. Ordered by increasing zirconium content in at% Zr, a) 5 at% Zr AZ055 at% Zr AZ05, b) 10 at% Zr AZ10, c) 15 at% Zr AZ15, d) 20 at% Zr AZ20.

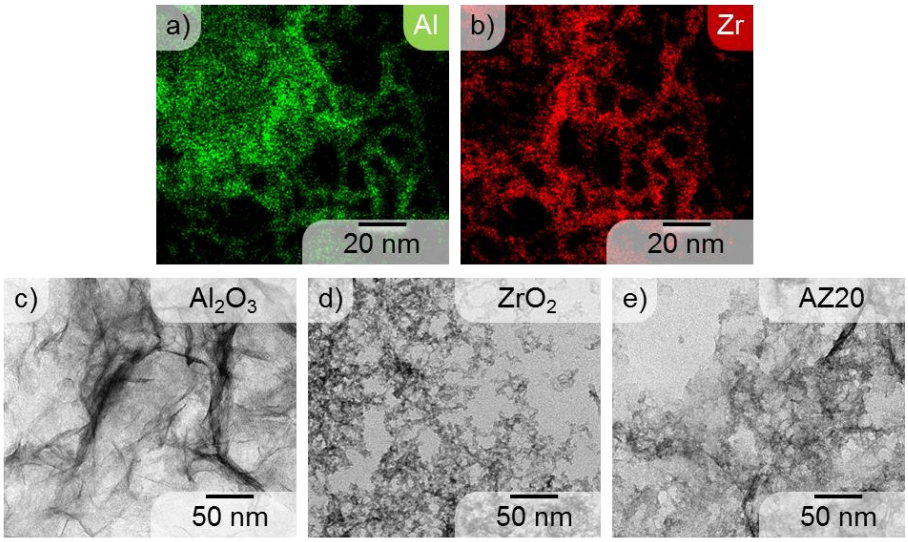

Figure S10: a) Aluminum and b) zirconium distributions for the field of view shown in figure 6. Bright-field TEM images of c) pure alumina aerogel, d) pure zirconia aerogel and e) AZ20 aerogel after annealing at 300 °C

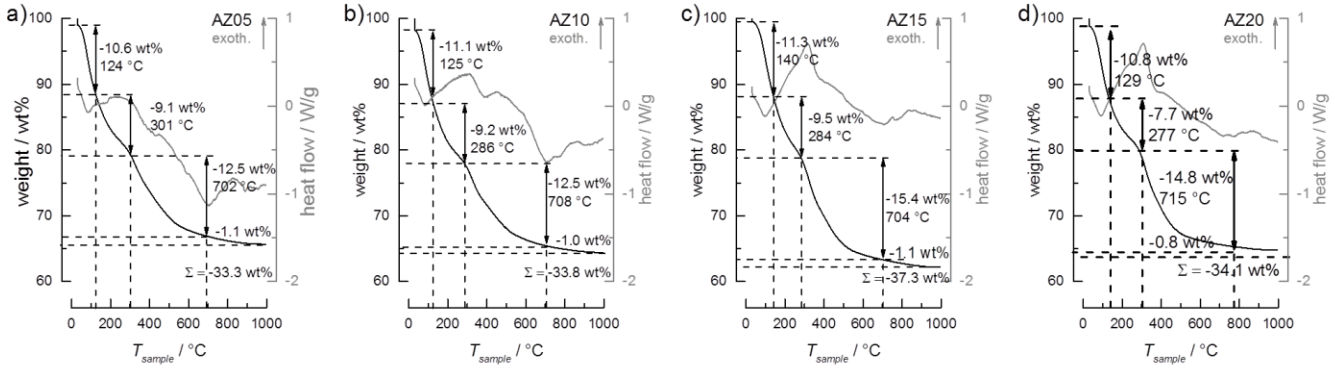

Figure S11: DTA-TG measurements of alumina mixed with zirconia (AZ) aerogels; Ordered by increasing zirconium content in at% Zr, a) 5 at% Zr AZ05, b) 10 at% Zr AZ10, c) 15 at% Zr AZ15, d) 20 at% Zr AZ20. While temperature of second step is decreasing the DTA signal is increasing in reason of earlier organic decomposition of zirconia.

Table S5. Enhanced mechanical properties of alumina zirconia aerogels and characterization; Young's modulus E, density ρ, specific Young's modulus E/ρ, specific surface area SSA, total pore volume TPV (at $p/p_o = 0.95$), shrinkage and compressive strength at 50% strain CS50.

Al_2O_3 : Zr / at% Zr	E / MPa	ρ / mg mL^{-1}	E/ρ / MPa mL g^{-1}	SSA / m^2 g^{-1}	TPV / cm^3 g^{-1}	shrinkage / %	CS50 / MPa
0	2.90 ± 0.18	49.8 ± 0.5	58 ± 3	709	1.25	29.2 ± 0.2	1.12 ± 0.04
5	4.70 ± 0.11	65.9 ± 1,9	71 ± 1	696	1.34	33.6 ± 0.6	1.77 ± 0.04
10	7.62 ± 0.15	85.8 ± 1.7	89 ± 0.3	602	1.36	38.7 ± 0.6	2.57 ± 0.11
15	8.92 ± 0.05	94.8 ± 3.7	94 ± 3	599	1.29	39.6 ± 1.0	3.50 ± 0.15
20	10.82 ± 0.76	86.6 ± 0.5	125 ± 9	508	1.16	34.1 ± 0.1	3.51 ± 0.34

REFERENCES

(S1) Alaoui, A. H.; Woignier, T.; Scherer, G. W.; Phalippou, J. Comparison between Flexural and Uniaxial Compression Tests to Measure the Elastic Modulus of Silica Aerogel. *J. Non. Cryst. Solids* **2008**, *354* (40–41), 4556–4561.